Biomath Communications
www.biomathforum.org/biomath/index.php/conference

Numerical Simulations for Chemotaxis Models

Gurgen Dallakyan
H.Emin 123, Russian-Armenian (Slavonic) University
dallakyangurgen@gmail.com

Abstract. In the paper, we study the usage of numerical methods in solution of mathematical models of biological problems. More specifically, Keller-Segel type chemotaxis models are discussed, their numerical solutions by sweep and Lax-Friedrichs methods are obtained and interpreted biologically.

Keywords: mathematical models, chemotaxis, numerical solution

1. Introduction

From microscopic bacteria through to the largest mammals, the survival of many organisms is dependent on their ability to navigate within a complex environment through the detection, integration and processing of a variety of internal and external signals. This movement is crucial for many aspects of behavior, including the location of food sources, avoidance of predators and attracting mates. The ability to migrate in response to external signals is shared by many cell populations, playing a fundamental role coordinating cell migration during organogenesis in embryonic development and tissue homeostasis in the adult. An acquired ability of cancer cells to migrate is

Citation: Gurgen Dallakyan, Numerical Simulations for Chemotaxis Models, Biomath Communications 6, pp. 16-33,
https://doi.org/10.11145/bmc.2019.04.277

believed to be a critical transitional step in the path to tumor malignancy. The directed movement of cells and organisms in response to chemical gradients, chemotaxis, has attracted significant interest due to its critical role in a wide range of biological phenomenon (the book of Eisenbach [1] provides a detailed biological comparison between chemotactic mechanisms across different cells and organisms).

Extensive research has been conducted into the mechanistic and signaling processes regulating chemotaxis in bacteria, particularly in E. coli [2], and in the life cycle of cell slimemolds such as Dictyostelium discoideum [3]. While the biochemical and physiological bases are less well understood, chemotaxis also plays a crucial role in the navigation of multicellular organisms. The nematode worm C. elegans undergoes chemotaxis in response to a variety of external signals [4] while in insects, the fruit fly Drosophila melanogaster navigates up gradients of attractive odours during food location [5] and male moths follow pheromone gradients released by the female during mate location [6].

Theoretical and mathematical modeling of chemotaxis dates to the pioneering works of Patlak in the 1950s and Keller and Segel in the 1970s. The review article by Horstmann [7] provides a detailed introduction into the mathematics of the KellerSegel (KS) model for chemotaxis. In its original form this model consists of four coupled reaction-advection-diffusion equations. These can be reduced under quasi-steady-state assumptions to a model for two unknown functions u and v. The general form of the model is

$$\begin{aligned} u_t =& \nabla(k_1(u,v)\nabla u - k_2(u,v)u\nabla v) + k_3(u,v), \\ v_t =& D_v\Delta v + k_4(u,v) - k_5(u,v)v, \end{aligned} \tag{1}$$

where u denotes the cell (or organism) density on a given domain $\Omega \subset R^n$ and v describes the concentration of the chemical signal. The cell dynamics derive from population kinetics and movement, the latter comprising a diffusive flux modeling undirected (random) cell migration and an advective flux with velocity dependent on the gradient of the signal, modeling the contribution of chemotaxis. $k_1(u,v)$ describes the diffusivity of the cells (sometimes also called motility) while $k_2(u,v)$ is the chemotactic sensitivity; both functions may de-

pend on the levels of u and v. k_3 describe cell growth and death while the functions $k_4$and k_5 are kinetic functions that describe production and degradation of the chemical signal. A key property of the above equations is their ability to give rise to spatial pattern formation when the chemical signal acts as an auto-attractant, that is, when cells both produce and migrate up gradients of the chemical signal.

2. Chemotaxis Models

Whilst a number of further approaches have been developed (e.g. stochastic and discrete approaches such as those in [8-12]), it is the deterministic KellerSegel continuum model that has become the prevailing method for representing chemotactic behavior in biological systems on the population level. A large amount of effort has been expended on explaining their origin from a mechanistic/microscopic description of motion. The review by Horstmann [7] considers five methods in detail. As mentioned above, KellerSegel type equations have become widely utilized in models for chemotaxis, a result of their ability to capture key phenomenon, intuitive nature and relative tractability (analytically and numerically) as compared to discrete/individual based approaches. Models based on the KellerSegel equations have also been developed to understand whether chemotaxis may underpin embryonic pattern forming processes, such as the formation and dynamics of the primitive streak (an early embryonic structure that coordinates tissue movements) [13]. In addition to their utilization within models for biological systems, a large body of work has emerged on the mathematical properties of the KellerSegel equations (1) and, in particular, on the conditions under which specialization or variations of (1) either form finite-time blow-up or have globally existing solutions. Childress and Percus [14] work has been devoted to a special case of (1), in which the functions k_j are assumed to have linear form, a model referred to as the *minimal model*.

The minimal model is derived according to a limited set of conjectures and a number of variations have been described based on additional biological realism. In this thesis, we consider some of these

variations. The variations are each introduced in a form that includes a single additional parameter that, under an appropriate limit, reduces the system to the minimal form. In many cases this modification regularizes the problem such that solutions exist globally in time. Hence we call the corresponding parameter for each of the extended models the regularization parameter. The regularization parameter allows us to study in detail bifurcation conditions, pattern formation and properties of the nonuniform solutions. We will not discuss certain questions such as the convergence of solutions of the variations to the minimal model in the corresponding limit.

Now it's the time to talk about variables figuring in chemotaxis models. Let's consider first three variables: the cell density, n, the chemoattractant concentration, c, and the stimulant concentration, s. The bacteria diffuse, move chemotactically up gradients of the chemoattractant, replicate and become non motile. The non motile cells can be thought of as dead, for the purpose of the model. The chemoattractant diffuses, and is produced and ingested by the bacteria. The stimulant diffuses and is consumed by bacteria. Below we list five chemotaxis models.

The minimal model

$$\begin{aligned} u_t =& \nabla(D\nabla u - \chi\,\nabla v)\,, \\ v_t =& \nabla^2 v + u - v \end{aligned} \qquad \text{(Model 1)}$$

Signal-dependent sensitivity models
Two versions of signal-dependent sensitivity, the "receptor" model,

$$\begin{aligned} u_t =& \nabla\left(D\nabla u - \frac{\chi\,u}{(1+\alpha\,v)^2}\,\nabla v\right), \\ v_t =& \nabla^2 v + u - v, \end{aligned} \qquad \text{(Model 2a)}$$

where for $\alpha \to 0$ the minimal model is obtained, and the "logistic" model

$$\begin{aligned} u_t =& n\nabla\left(D\nabla u - \chi\,u\frac{1+\beta}{v+\beta}\,\nabla v\right), \\ v_t =& \nabla^2 v + u - v \end{aligned} \qquad \text{(Model 2b)}$$

where for $\beta \to \infty$ the minimal model follows and for $\beta \to 0$ we obtain the classical form of $\chi(v) = 1/v$.

Density-dependent sensitivity models
Two models with density-dependent sensitivity, the "volume-filling" model,

$$\begin{aligned} u_t =& \nabla \left(D\nabla u - \chi\, u \left(1 - \frac{u}{\gamma}\right) \nabla v \right), \\ v_t =& \nabla^2 v + u - v \end{aligned} \qquad \text{(Model 3a)}$$

where the limit of $\gamma \to \infty$ leads to the minimal model, and

$$\begin{aligned} u_t =& \nabla \left(D\nabla u - \chi\, u \left(1 - \frac{u}{\gamma}\right) \nabla v \right), \\ v_t =& \nabla^2 v + u - v, \end{aligned} \qquad \text{(Model 3b)}$$

where $\varepsilon \to 0$ leads to the minimal model, and finally

$$\begin{aligned} u_t =& \nabla \left(D u^n \nabla u - \chi\, u\, \nabla v \right), \\ v_t =& \nabla^2 v + u - v \end{aligned}$$

where the minimal model corresponds to the limit of $n \to 0$.

The nonlinear signal kinetics model

$$\begin{aligned} u_t =& \nabla \left(D\nabla u - \chi\, u\, \nabla v \right), \\ v_t =& \nabla^2 v + \frac{u}{1 + \varphi\, u} - v, \end{aligned} \qquad \text{(Model 4)}$$

which approximates the minimal model for $\varphi \to 0$.

The cell kinetics model

$$\begin{aligned} u_t =& \nabla \left(D\nabla u - \chi\, u\, \nabla v \right) + ru(1-u), \\ v_t =& \nabla^2 v + u - v \end{aligned} \qquad \text{(Model 5)}$$

which in the limit of zero growth, $r \to 0$, leads to the minimal model.

Parabolic models of chemotaxis
Another version of the Keller-Segel type model describes the evolution of the density $\rho(x,t)$, $t \geq 0$, $x \in R^d$ of one type of cells and the concentration $\varphi(x,t)$ of the chemical attracting substance. A general form of the system reads

$$\begin{cases} \rho_t = \nabla \cdot (\nabla P(\rho)) - \nabla \cdot (\rho\, \chi\,(\rho, \varphi)\, \nabla \varphi) \\ \varphi_t = D\Delta\varphi + a\rho - b\varphi \end{cases} \tag{2}$$

The motion of cells is described by a continuity equation in which the flux is biased by diffusion and chemotactic transport up to a gradient of a nutrient. Denoting the velocity of cells as $\vec{u}$, the flux equals $\rho\,\vec{u} = -\nabla(P(\rho)) + \chi\,(\rho)\,\nabla\varphi$. Here P denotes a nonlinear diffusion function due to the presence of a density dependent random mobility for the cells, while $\chi(\rho,\varphi)$ is a chemosensitivity function and describes the response of cells to the presence of chemoattractant. Considering different forms of these functions we can obtain many variations of the above model.

Typical examples for the function $P(\rho)$ defining the diffusive flux are given by

- Fick's law (classical linear diffusion): $P(\rho) = \varepsilon\rho$, $\varepsilon > 0$
- Darcy's law (porous medium type diffusion): $P(\rho) = \varepsilon\rho^\gamma$, $\varepsilon > 0$, $\gamma > 1$.

The porous medium type diffusion reflects the density dependent random motility, which models volume filling effects due to the finite volume and finite compressibility of cells [15],[16],[17]. In the case of the chemosensitivity function the simplest form corresponds to the sensitivity of cells independent on the concentration of the chemical, i.e. $\chi(\rho,\varphi) = \chi_0$ is constant, where $\chi_0 > 0$ for positive chemotaxis. However, various modifications were introduced to model quorum sensing, volume filling or signal limiting responses. For example

- Signal dependent sensitivity function:
  - "receptor": $\chi(\rho,\varphi) = \dfrac{\chi_1}{(\chi_2 + \varphi)^2}$, $\chi_1, \chi_2 > 0$,

– "logistic": $\chi(\rho,\varphi) = \dfrac{\chi_1+\chi_2}{\chi_0+\varphi}$, $\chi_0 > 0$

- Density dependent sensitivity function ("volume filling"):

$$\chi(\rho,\varphi) = \chi_0(1-\frac{\rho}{\rho_{\max}}), \quad \chi_0,\, \rho_{\max} > 0$$

One of the characteristic features of the system (2) is the balance between pressure forces, which are modeled by diffusion, and chemotaxis. More precisely, expanding the equation for ρ in (2) with constant function $\chi(\rho,\varphi) = \chi$ we get

$$\rho_t = \Delta P(\rho) - \rho\,\chi\,\Delta\varphi - \chi\,\nabla\rho\,\nabla\varphi.$$

Contribution of the "Laplacian" terms have different signs. This suggests to think of diffusion as stabilizing force, while chemotaxis can be seen to have a destabilizing effect. Balance between these two processes can result in some steady spatial patterns in ρ and φ, or in some unsteady traveling wave solutions. On the other hand, if the chemotactic force is sufficiently strong, there is a possibility of a blow-up of solutions in finite time. The blow-up of solutions may in fact can happen, for example in a simplified version of Keller-Segel type model in two space dimensions, where the parabolic equation for the concentration of chemical is substituted by an elliptic one and the decay of φ is dropped. If the initial mass is larger than some threshold values, then the solution concentrates into a Diracs delta in finite time.

The blow-up phenomenon is sometimes considered as the weakens of the classical Keller- Segel system. This motivates the introduction of nonlinear diffusion $P(\rho)$ and chemosensitivity function $\chi(\rho,\,\varphi)$, to achieve a more refined balance between diffusion and chemotaxis and guarantee the global existence of solution.

Macroscopic, parabolic type of models describe very well the aggregation phenomenon but fail when the network structures have to be reproduced. This was observed while studying the experiments on the vasculogenesis process. The Patlak-Keller-Segel model cannot explain this process as well as cannot describe the "run and tumble" movement

of, for example, Eusterichia Coli. This is because it is mainly directed to the long time scales evolutions. As a consequence, in recent years there is a tendency to use hyperbolic systems, which correspond to models at the lower, mesoscopic scale. The main difference between the two approaches is that diffusion systems describe the evolution via the density of the population whereas hyperbolic models are based on the individual movement behavior. They take into account the fine structure of the problem and are able to capture the particular features of the modeled quantity. Moreover, they account for finite propagation speed. Lower level of description implies also that some relevant model parameters, for example turning rates, can be measured from the individual movement patterns. This results in more realistic description on phenomenon occurring at short time scales. This two classes of systems are linked by long time asymptotics.

3. Numerical Solutions of Chemotaxis Models

Difference scheme

Finding an analytical solution to a system of partial differential equations is not trivial, and may not always be intuitively revealing. Thus we seek numerical approximations to the PDEs. A finite difference method replaces partial derivatives with approximations, which creates a finite dimensional system that can be solved using a computer. There are various finite difference schemes with different orders of accuracy.

Consider one-dimensional parabolic-elliptic KS model

$$\frac{\partial u}{\partial t} = u_{xx} - \chi \left(u v_x\right)_x , \; u(x,0) = u_0(x) \geq 0 , \; 0 < l < x , \; 0 < t < T \tag{3}$$

$$v_{xx} = -u , \; 0 < x < l , \; 0 < t < T \tag{4}$$

$$u(0,t) = \phi(t) , \; u(l,t) = \psi(t) , \; v(0,t) = \mu(t) , \; v(l,t) = \nu(t) , \; 0 < x < l. \tag{5}$$

To build a difference scheme of the system (3) - (5), we require that the functions $u(x,t)$, $v(x,t)$ are sufficiently smooth. We introduce an

even grid with step h in variable x and step τ in t , i.e.

$$\omega_h = \{x_j = jh\,,\ j = 0,\ 1, \ldots, N\,,\ h\,N = l\,\}$$
$$\omega_\tau = \{\,t_n = n\tau\,,\ j = 0,\ 1, \ldots, K\,,\ \tau\,K = T\,\}$$

The difference scheme corresponding to system (3) - (5) has the following form

$$\frac{y_j^{n+1} - y_j^n}{\tau} = \frac{y_{j+1}^n - 2y_j^n + y_{j-1}^n}{h^2} - \chi\frac{(y_{j+1}^n - y_{j-1}^n)}{2h}\frac{(z_j^n - z_{j-1}^n)}{h} - \quad (6)$$
$$-\,\chi\,y_j^n\,\frac{z_{j+1}^n - 2z_j^n + z_{j-1}^n}{h^2}\,,\ j = 1, \ldots, N-1\,,\ n = 0, \ldots, K-1$$

$$y_j^0 = u_0(x_j),\ , j = 0, 1, \ldots, N,\ y_0^n = \phi(t_n),\ y_N^n = \psi(t_n),\ , n = 0, 1, \ldots, K,$$

$$\frac{z_{j-1}^n - 2z_j^n + z_{j+1}^n}{h^2} = -y_j^n,\ j = 1, ..., N-1\,,\ n = 0, ..., K-1 \quad (7)$$
$$z_0^n = \mu(t_n)\,,\ z_N^n = \nu(t_n)\,,\ n = 0,\ 1, \ldots, K.$$

This is an explicit difference scheme. Here the difference equation (6) approximates the differential equation (3) at the point (x_j, t_n) with the first order in $\tau$and the second order in h. The difference equation (7) approximates the differential equation (4) at the point (x_j, t_n) with second order in h.

Note, that difference scheme (7) has a tridiagonal matrix, so it can be solved by the sweep method, which is a partial version of Gauss elimination method. Recall, that for the systems of linear algebraic equations with a tridiagonal matrix

$$a_j y_{j-1} - c_j y_j + b_j y_{j+1} = -f_j\,,\ j = 1, 2, ...N-1,$$
$$y_0 = k_1 y_1 + \mu_1\,,\ y_N = k_2 y_{N-1} + \mu_2$$

conditions of stability for the sweep method look like this

$$a_j \neq 0\,,\ b_j \neq 0\,,\ |\,c_j| \geq |a_j| + |b_j|\ ,\ j = 1, 2, \ldots, N-1,$$
$$|k_1| \leq 1\,,\ |k_2| < 1$$

It is proved in classical books in numerical methods, that schemes like (6), (7) are conditionally stable for each fixed n and they can be solved by the sweep method starting from $n = 0$.

When solving the scheme (6), (7), we apply the principle of frozen coefficients. Suppose, that

$$z_j^n - z_{j-1}^n = \xi_j^n = const,$$
$$z_{j-1}^n - 2z_j^n + z_{j+1}^n = \delta_j^n = const.$$

Then the difference scheme (6), (7) gets the following form

$$\frac{y_j^{n+1} - y_j^n}{\tau} = \frac{y_{j+1}^n - 2y_j^n + y_{j-1}^n}{h^2} - \chi\xi_j^n \frac{y_{j+1}^n - y_{j-1}^n}{2h^2} - \frac{\chi\delta_j^n}{h^2} y_j^n ,$$
$$j = 1, \ldots, N-1 \, , \, n = 0, \ldots, K-1$$
$$y_j^0 = u_0(x_j) \, , \, j = 0, 1, \ldots, N, \, y_0^n = \phi(t_n), \, y_N^n = \psi(t_n) \, , \, n = 0, 1, \ldots, K.$$

Thus, the system of difference schemes (6), (7) can be solved as follows:

1) find the values of z_j^0 on the zero layer from the difference scheme (7);

2) find the values of y_j^1 on the first layer from the difference scheme (6), using the values of z_j^0 , δ_j^0 , ξ_j^0 and y_j^0:

$$y_j^1 = (1 - 2\eta - \chi\eta\delta_j^0)y_j^0 + (\eta + \frac{1}{2}\chi\tau\eta\xi_j^0)y_{j-1}^0 + (\eta - \chi\tau\eta\xi_j^0)y_{j+1}^0,$$

where $\eta = \frac{\tau}{h^2}$;

3) find the values of z_j^1 on the first layer from the difference scheme (7), using the values y_j^1.

It can be proved that this scheme is conditionally stable. And this is significant drawback of this scheme. Below the result of the C++ code for this simulation is presented (figure 1).

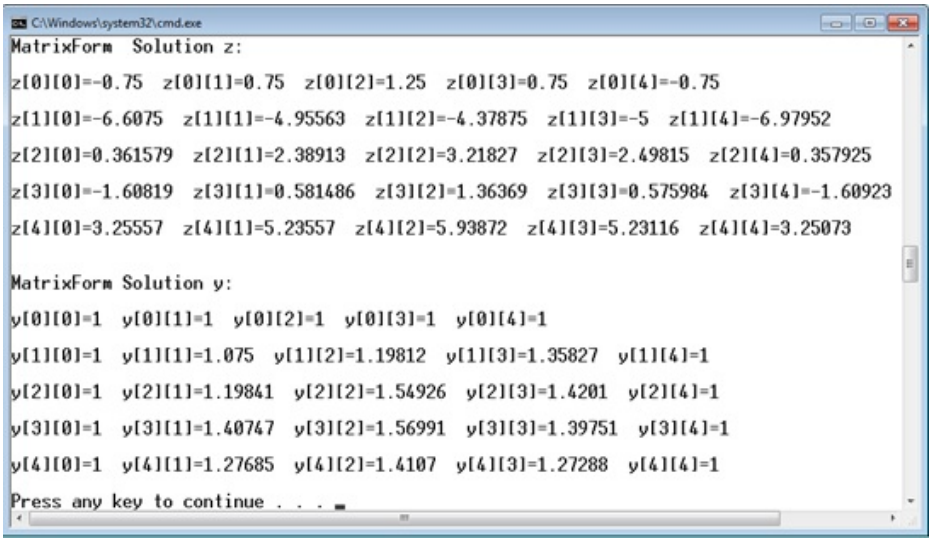

Figure 1: Sweep method implementation result

Lax-Friedrichs method

The Lax-Friedrichs (LxF) method [18], [19] is a basic method for the solution of hyperbolic partial differential equations. Its use is limited because its order is only one, but it is easy to program, applicable to general PDEs, and has good qualitative properties because it is monotone.

In this section we apply the second order Lax-Friedrichs scheme to simulate the KS-type liquid model found in Tyson [20]. The parameters of the KS equations of the model are also taken from [20]. Consider the simplest liquid model

$$\begin{cases} \dfrac{\partial u}{\partial t} = d_u u_{xx} - \alpha \left[\dfrac{u}{(1+v)^2} v_x \right]_x, \quad x \in [a,b]\,,\ t > 0 \\ \dfrac{\partial v}{\partial t} = v_{xx} + \dfrac{u^2}{\mu + u^2} \end{cases} \tag{8}$$

Again u represents cell density, v represents the chemoattractant concentration defining cell movement in response to chemical gradients, α is the chemotaxis coefficient, μ is the saturation level of chemoattractant production and d_u is the diffusion ratio between cells and

chemoattractant [20]. This simple liquid model implies a uniform distribution of the stimulant, which remains constant throughout the experiment.

According to LxF scheme the solution of a PDE is approximated on a mesh with constant increments Δx in space and Δt in time: $u_m^n \approx u\,(m\Delta x\,,\, n\Delta t)$. For the one-way wave equation (Burgers equation) $u_t + au_x = 0$, the LxF method is

$$\frac{u_m^{n+1} - 0.5(u_{m+1}^n + u_{m-1}^n)}{\Delta t} + a\frac{u_{m+1}^n - u_{m-1}^n}{2\Delta x} = 0$$

The numerical solution converges as the increments go to zero if

$$\left| a\,\frac{\Delta t}{\Delta x} \right| = |a\lambda| \leq 1.$$

In LxF method the key observation is that the approximations u_j^{n+1} with odd indices j are computed using only approximations u_j^n with even indices i and vice versa. The method computes u_m^{n+1} by first using u_{m-1}^n and u_m^n to take a half step in both space and time with LxF to get $u_{m-1/2}^{n+1/2}$ and similarly uses u_m^n and u_{m+1}^n to get $u_{m+1/2}^{n+1/2}$. These two first order results are then used along with u_m^n to compute a second order result u_m^{n+1}. If we take another half step with LxF instead of a whole step, we get a first order result u_m^{n+1} and a method that we call the two-step LxF method. Thus our LxF scheme for the system (9) is given by,

$$\begin{cases} u_j^{n+1} = u_j^n - \alpha\dfrac{\Delta t}{\Delta x}\left[\,\overset{)}{f}_{j+\frac{1}{2}} - \overset{)}{f}_{j-\frac{1}{2}}\right] + \dfrac{d_u\,\Delta t}{\Delta x^2}\left[u_{j+1}^n - 2u_j^n + u_{j-1}^n\right] \\ v_j^{n+1} = v_j^n + \dfrac{\Delta t}{\Delta x^2}\left[v_{j+1}^n - 2v_j^n + v_{j-1}^n\right] + \Delta t\dfrac{(u_j^n)^2}{\mu + (u_j^n)^2} \end{cases} \tag{9}$$

where the numerical flux defined at $x_{j\pm\frac{1}{2}}$ is,

$$\overset{)}{f}_{j\pm\frac{1}{2}} = \frac{1}{2}\left[f(u_{j\pm\frac{1}{2}}^-) + f(u_{j\pm\frac{1}{2}}^+) - \alpha_{j\pm\frac{1}{2}}(u_{j\pm\frac{1}{2}}^+ - u_{j+\frac{1}{2}}^-)\right].$$

Note that

$$f(u^-_{j\pm\frac{1}{2}}) \approx \frac{p_{j\pm\frac{1}{2}}}{(1+v_{j\pm\frac{1}{2}})^2}\, u^-_{j\pm\frac{1}{2}},$$

$$f(u^+_{j\pm\frac{1}{2}}) \approx \frac{p_{j\pm\frac{1}{2}}}{(1+v_{j\pm\frac{1}{2}})^2}\, u^+_{j\pm\frac{1}{2}},$$

$$\alpha_{j+\frac{1}{2}} = \left| \frac{(v_x)_{j+\frac{1}{2}}}{\left(1+v_{j+\frac{1}{2}}\right)^2} \right|,$$

where

$$p_{j+\frac{1}{2}} = \frac{(v_x)_j - (v_x)_{j+1}}{2},$$
$$v_{j+\frac{1}{2}} = \frac{v_j + v_{j+1}}{2}$$

and

$$u^+_{j+\frac{1}{2}} = \frac{3u_{j+1} - u_{j+2}}{2},$$
$$u^-_{j+\frac{1}{2}} = \frac{3u_j - u_{j-1}}{2}.$$

Instead of periodic boundary conditions here we enforce zero Neumann boundary conditions. We have $x \in [a, b]$, thus the boundary conditions take the form,

$$u_x(a,t) = u_x(b,t) = 0$$
$$(v_x)_{j=1} = (v_x)_{j=M+1} = 0$$

We apply $u_x(x=a,t) \approx \frac{u_2-u_1}{\Delta x} = 0$ and $u_x(x=b\,,t) \approx \frac{u_{M+1}-u_M}{\Delta x} = 0$, therefore at all the time level we apply the following zero Neumann boundary condition, $u_{M+1} = u_M$, $u_1 = u_2$. Similarly we have $v_{M+1} = v_M$, $v_1 = v_2$ for the chemotaxis variable.

Numerical simulation

We execute a numerical test on the liquid model (8) with the Lax-Friedrichs scheme (9). The initial condition for the cell density is

taken as $u(x,0) = u_0 + r_p$ with $u_0 = 1$ and randomized perturbation of size $r_p = 10^{-1}$. The initial condition for the chemical concentration is $v(x,0) = 0$. The computational domain is $[a;b] = [0;10]$. The time step size used is $\Delta t = \frac{1}{4}\Delta x^2$ with total mesh points $M = 25$. The parameter values used in system (8) are $\alpha = 0$, $\mu = 1$, $d_u = 0.33$. Initial conditions and parameter values were taken from Tyson [20]. Below the result of the Wolfram Mathematica code for this simulation is presented (figure 2).

The results of this simulation can be seen in the figure 2. Since the cells are randomly distributed throughout the domain, we initially see many peaks and troughs in cell density. At this point the cells have just begun to secrete chemoattractant.

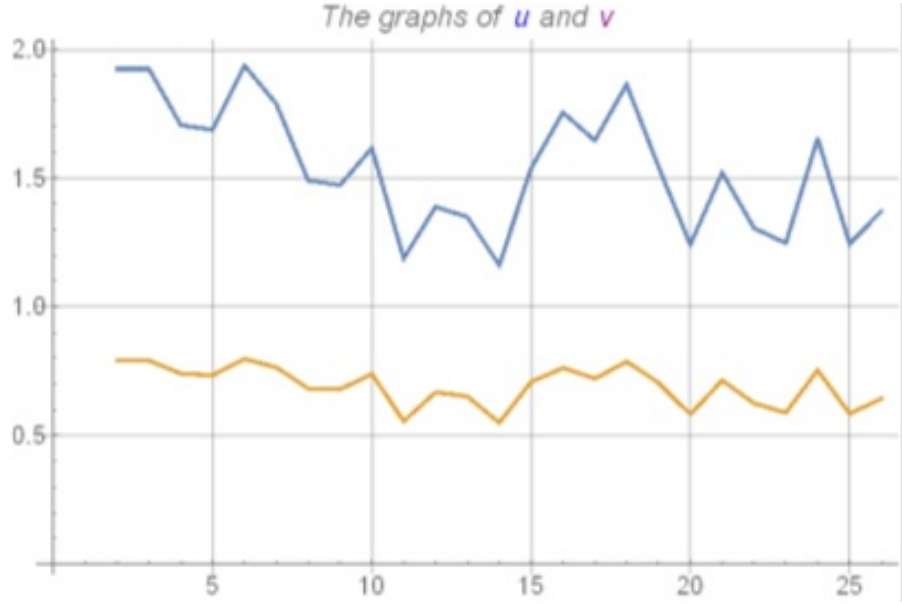

Figure 2: Sweep method implementation result

Biological interpretation

As time moves on the cells continue to produce chemoattractant. In figure 2 we see that the many initial peaks in cell density have quickly given way to a lesser number of peaks with increased amplitudes. The

difference in amplitudes can be explained by competition between the cell groups. A group of cells with higher density will produce more chemoattractant than a group of cells with lower density, thus attracting cells to the higher density group at a faster rate.

As time continues to move on, we see a reduction in the number of peaks in cell density. While the populations of high cell density continue to produce high levels of chemoattractant, diffusion is working against them, dissipating the concentrations of chemoattractant. If a group of cells is not producing enough chemoattractant to overpower the diffusion process that group will start to lose cell population to a group of cells whose chemoattractant production surpasses the diffusion rate. Thus we see a reduction in the number of populations with high cell density.

We see also the further effects of competition between groups of cells. Again the number of populations of high cell density is reduced, with one group out-pacing the other in cell density. Since the amount of chemoattractant in the dish has no way to dissipate, eventually cells saturate and their movement is no longer governed by chemotaxis. The process of diffusion will then take over, meaning cells will travel down the concentration gradient to areas of lesser cell density.

Conclusion

The aim of this work was to analyze and solve particular mathematical models describing the phenomenon of chemotaxis. Since the cells density depends on the nutrient concentration and vice versa, there exists a coupling between equations describing their evolution in time. The considered models have the form of a system of ordinary and partial differential equations of a reaction-diffusion type. These kinds of system play an important role in cancer modeling.

These so-called multiscale models are far more accessible to the biologist both in terms of understanding and in terms of experimental validation. Mathematical models of cancer are often complex and are unlikely to be amenable to standard mathematical analysis and therefore are nearly always solved by means of computational solution.

Such computational solutions, either numerical or simulation-based, require a great deal of computing power, which has only recently become widely available. It seems clear that we have now seen the emergence of computational models as the dominant tool in mathematical models of chemotaxis. In presented work, two main results can be mentioned:

1. One Keller-Segel type model of chemotaxis is solved numerically by means of sweep method.

2. One, Keller-Segel type liquid model is solved numerically by Lax-Friedrichs method. Then the results (also Wolfram illustrations) are interpreted biologically.

In future, a peculiar numerical and mathematical analysis for gradient-based slope limiters for the partial differential equations on surfaces is desired. We are optimistic that this is a very promising stabilization method for the numerical treatment of surface-based chemotaxis problems in medicine and biology.

References

[1] M. Eisenbach. Chemotaxis. Imperial College Press, London, 2004.

[2] M.D. Baker, P.M. Wolanin, J.B. Stock, *Signal transduction in bacterial chemotaxis*, Bioessays **28**(1), 922, 2006.

[3] D. Dormann, C.J. Weijer, *Chemotactic cell movement during Dictyostelium development and gastrulation*, Curr. Opin. Genet. Dev. **16**(4), 367373, 2006.

[4] H.G. Othmer, S.R. Dunbar, W. Alt, *Models of dispersal in biological systems*, J. Math. Biol. **26**, 263298, 1988.

[5] S.A. Budick, M.H. Dickinson, *Free-ight responses of Drosophila melanogaster to attractive odors*, J. Exp. Biol. **209**(15), 30013017, 2006.

[6] J.S. Kennedy, D. Marsh, *Pheromone-regulated anemotaxis in ying moths*, Science **184**, 9991001, 1974.

[7] D. Horstmann, *From 1970 until present: the KellerSegel model in chemotaxis and its consequences*, I. Jahresberichte DMV **105**(3), 103165, 2003.

[8] J.C. Dallon, H.G. Othmer, *A discrete cell model with adaptive signaling for aggregation of dictyostelium discoideum*, Philos. Trans. R. Soc. B **352**, 391417, 1997.

[9] E. Jabbarzadeh, C.F. Abrams, *Chemotaxis and random motility in unsteady chemoattractant elds: a computational study*, J. Theor. Biol. **235**(2), 221232, 2005.

[10] A.F. Maree, P. Hogeweg, *How amoeboids self-organize into a fruiting body: multicellular coordination in Dictyostelium discoideum*, Proc. Natl. Acad. Sci. USA **98**(7), 38793883, 2001.

[11] N. Mittal, E.O. Budrene, M.P. Brenner, *Van Oudenaarden, A. Motility of Escherichia coli cells in clusters formed by chemotactic aggregation*, Proc. Natl. Acad. Sci. USA **100**(23), 1325913263, 2003.

[12] E. Palsson, H.G. Othmer, *A model for individual and collective cell movement in Dictyostelium discoideum*, Proc. Natl. Acad. Sci. USA **97**(19), 10581063, 2000.

[13] K.J. Painter, P.K. Maini, H.G. Othmer, *Complex spatial patterns in a hybrid chemotaxis reaction-diffusion model*, J. Math. Biol. **41**(4), 285314, 2000.

[14] S. Childress, J.K. Percus, *Nonlinear aspects of chemotaxis*, Math. Biosci. **56**, 217237, 1981.

[15] V. Calvez, J. A. Carrillo, *Volume effects in the Keller-Segel model: energy estimates preventing blow-up*, J. Math. Pures Appl. (9), **86**(2):155175, 2006.

[16] R. Kowalczyk, *Preventing blow-up in a chemotaxis model*, J. Math. Anal. Appl., **305**(2):566588, 2005.

[17] L.F. Shampine, *Two-step Lax-Friedrichs method*, Applied Mathematics Letters Volume 18, Issue 10, October 2005, Pages 1134-1136.

[18] T. Darvishi, Norollah Darvishi, *SOR-Steffensen-Newton method to solve systems of nonlinear equations*, Applied Mathematics, **2**(2), 2127, 2012.

[19] Francis Filbet, Philippe Laurencot, Beno t Perthame, *Derivation of hyperbolic models for chemosensitive movement*, J. Math. Biol. **50**(2):189207, 2005.

[20] R. Tyson. Pattern Formation by E. Coli; Mathematical and numerical investigation of a biological phenomenon. PhD thesis, University of Washington.